Available online at www.sciencedirect.com

ScienceDirect

Procedia Structural Integrity 13 (2018) 578–583

Structural Integrity Procedia

www.elsevier.com/locate/procedia

ECF22 − Loading and Environmental effects on Structural Integrity

Crack initiation of selected geopolymer mortars with hemp fibers

Hana Simonova[a,*], Barbara Kucharczykova[a], Libor Topolar[a], Zbynek Kersner[a], Ildiko Merta[b], Jelena Dragas[c], Ivan Ignjatovic[c], Miroslav Komljenovic[d], Violeta Nikolic[d]

[a]*Brno University of Technology, Faculty of Civil Engineering, Veveri 331/95, 602 00 Brno, Czech Republic*
[b]*Technische Universität Wien, Faculty of Civil Engineering, Adolf-Blamauer-Gasse 1-3, 1030 Vienna, Austria*
[c]*University of Belgrade, Faculty of Civil Engineering, Bulevar kralja Aleksandra 73, 11000 Belgrade, Serbia*
[d]*University of Belgrade, Institute for Multidisciplinary Research, Kneza Višeslava 1, 11030 Belgrade, Serbia*

Abstract

The aim of this paper is to quantify particularly fracture properties of selected types of mortars prepared with an alkali activated binder and hemp fibers. The main attention is focused on evaluation of three-point bending fracture tests of prismatic specimens with an initial central edge notch made of alkali activated fly ash mortars. The load versus crack mouth opening displacement (*F–CMOD*) diagrams were recorded during the fracture tests and subsequently evaluated using the Double-*K* fracture model. This model allows the quantification of two different levels of crack propagation: initiation, which corresponds to the beginning of stable crack growth, and the level of unstable crack propagation. The course of fracture tests was also monitored by acoustic emission method.

Peer-review under responsibility of the ECF22 organizers.

Keywords: Geopolymer, hemp fibre, fracture test, acoustic emission, crack initiation, Double-*K* model.

1. Introduction

The manufacturing of cement is highly energy intensive because of the extreme heat required to produce it, resulting in high pollution, carbon dioxide (CO_2) emissions and consequently in global warming and climate change. Producing a ton of cement generates nearly a ton of CO_2 and alarmingly the cement industry alone emits around 7–10% of the total CO_2 on Earth (Aïtcin and Mindess (2011), Scrivener et al. (2016)). Since the cement production is permanently growing by 2.5% annually, these numbers will become even worse. For that reason, there is the increased effort to

* Corresponding author. Tel.: +420 541 147 381.
E-mail address: simonova.h@vutbr.cz

2452-3216
Peer-review under responsibility of the ECF22 organizers.
10.1016/j.prostr.2018.12.095

developed innovative environmental friendly building materials as an alternative to ordinary Portland cement-based concrete. The alkali activated materials (AAMs) belongs to a promising alternative to traditional cement (Provis and van Deventer (2014), Shi et al. (2006)). AAMs are solid calcium silicate or aluminosilicate materials (so-called geopolymers) formed by alkali activation of solid prime materials (metallurgical slags, coal combustion-based fly ashes, ground granulated blast furnace slag, etc.). The manufacture of AAMs emits up to 80% less CO_2 than that of the ordinary cement.

The same like cement concrete, AAMs also belongs to quasi-brittle materials with low energy absorption capacity under tensile load. To overcome this problem different types of steel or synthetic fibers are used in concrete. Environmentally guided trend of research leads the use of sustainable alternative to steel and synthetic materials. Naturally available fibers produced from different types of plants (e.g. hemp, flax) grown locally make a renewable, biodegradable and relatively cheap alternatives (Zhou and Kastiukas (2017)).

The works published in technical and research papers are currently focused on of AAMs but unfortunately limited information on the fracture properties of these composites is available in the literature (Sarker et al. (2013)). Therefore, the main attention of this paper is focused on the evaluation of three-point bending fracture tests of prismatic specimens with an initial central edge notch made of selected fly ash based geopolymer mortars reinforced with hemp fibers. Especially, the attention is paid to the quantification of two different levels of crack propagation using the Double-*K* fracture model (Reindhardt and Xu (1999), Kumar and Barrai (2011)). The initiation of cracks during the fracture tests was also monitored by the acoustic emission method, e.g. Grosee and Ohtsu (2008).

2. Experimental part

2.1. Material and specimens

The prism specimens with nominal dimensions 40 × 40 × 160 mm made of geopolymer mortars were studied. In total three set of specimens were tested. The first one was reference, designated as AAFAM, another two sets contained different volume percentage of hemp fibers (0.5 and 1.0 %), designated as AAFAM_0.5 and AAFAM_1.0, respectively. The power plant fly ash, sodium silicate solution as alkali activator, river sand with maximum grain size 8 mm, water and hemp fibers with length of 10 mm were used to produce the sets of specimens. All geopolymer mortar specimens were prepared according to the previously optimized procedure by Komljenovic et al. (2010). More details about mortars mix design, specimens' production and curing conditions can be found in Simonova et al. (2018).

2.2. Fracture tests

Based on the test requirements, the test specimens were before testing provided with an initial central edge notch and subsequently subjected to the fracture tests in the three-point bending configuration. The nominal depth of notch was about 1/3 of the specimen height and span length was set to 120 mm. The fracture tests were performed in very stiff multi-purpose mechanical testing machine LabTest 6-1000.1.10. The load range of testing machine is 0 to 1000 kN. The loading procedure was performed with the requirement of a constant increment of displacement which was set to 0.02 mm/min. In this way, the diagram of loading force F in relation to the crack mouth opening displacement *CMOD* during the fracture test was recorded. The *CMOD* value was measured using the extensometer (crack opening displacement transducer), placed between blades fixed close to the notch, connected to the HBM Quantum X data logger during the loading test. All measured parameters (time, loading force and crack mouth opening) were continuously recorded into the data logger with a frequency of 5 Hz.

All performed fracture tests were accompanied by the measurements using the acoustic emission (AE) technique. During the fracture tests, the AE signals were detected using four magnetic sensors (MDK-13) which were placed for all specimens at the same positions (two sensors on the upper surface, two sensors in the longitudinal axis of the specimen placed on its ends). The AE sensors were attached by magnets to the pre-prepared metal strips fixed by beeswax onto the surface of the individual specimens. Measured AE signals were amplified by a 35 dB amplifier and transmitted to the universal measuring and diagnostic system DAKEL-XEDO which was developed by the diagnostics department of Czech company DAKEL-ZD Rpety. This equipment allows recording and digital processing of AE signals. The overall fracture test configuration and positions of AE sensors can be seen in Fig. 1.

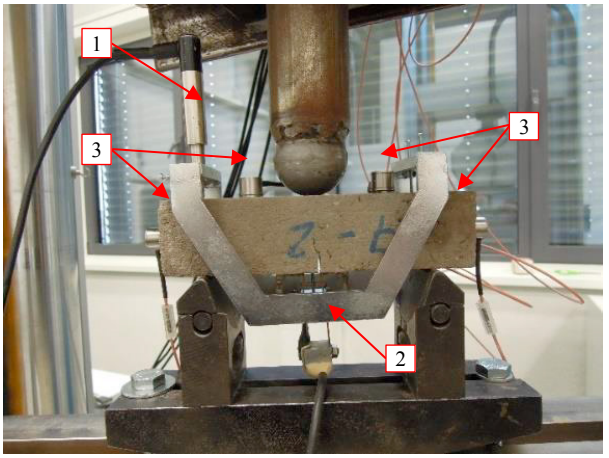

Fig. 1. Fracture test configuration: detail of the specimen with position of sensors (1 − deflection sensor fixed in the measurement frame, 2 − extensometer, 3 – AE sensors).

3. Double-*K* fracture model

The Double-*K* fracture model was utilized to evaluate mechanical fracture parameters from *F*−*CMOD* diagrams. In principle, this model combines the concept of cohesive forces acting on the faces of the fictitious (effective) crack increment with a criterion based on the stress intensity factor (details can be found in numerous publications – e.g. in Kumar and Barrai (2011). The advantage of this model is that it describes different levels of crack propagation: an initiation part which corresponds to the beginning of stable crack growth (at the level where the stress intensity factor, K_{Ic}^{ini}, is reached), and a part featuring unstable crack propagation (after the unstable fracture toughness, K_{Ic}^{un}, has been reached).

In this case, the unstable fracture toughness K_{Ic}^{un} was numerically determined first, followed by the cohesive fracture toughness K_{Ic}^{c}. When both of these values were known, the following formula was used to calculate the initiation fracture toughness K_{Ic}^{ini}:

$$K_{Ic}^{ini} = K_{Ic}^{un} - K_{Ic}^{c}. \tag{1}$$

Details regarding the calculation of both unstable and cohesive fracture toughness can be found e.g. in Kumar and Barrai (2011) or Zhang and Xu (2011). Calculation of parameter K_{Ic}^{un} is dependent on geometry function $F_1(\alpha)$ which is defined for the case of three-point bending configuration as:

$$F_1(\alpha) = \frac{1.99-\alpha(1-\alpha)(2.15-3.93\cdot\alpha+2.7\cdot\alpha^2)}{(1+2\cdot\alpha)(1-\alpha)^{3/2}}, \text{ and } \alpha = \frac{a_c}{D}, \tag{2}$$

where a_c is the critical effective crack length and D is the specimen depth.

Generally, in the cohesive crack model, the relation between the cohesive stress σ and the effective crack opening displacement COD is referred to as the cohesive stress function $\sigma(COD)$. The cohesive stress $\sigma(CTOD_c)$ at the tip of the initial notch of length a_0 at the critical state can be obtained from the softening curve. In this paper, bilinear softening curve was used. When using the bilinear softening curve, two cases may occur. In case I ($CTOD_c \leq COD_s$), $\sigma(CTOD_c)$ value can be determined according to the formula:

$$\sigma(CTOD_c) = f_t - (f_t - \sigma_s)\frac{CTOD_c}{COD_s}, \tag{3}$$

where f_t is the tensile strength, in this case determined by identification, see details in Šimonová et al. (2018), $CTOD_c$ is critical crack tip opening displacement, see e.g. Kumar and Barai (2011), σ_s and COD_s are the ordinate and abscissa

at the point of slope change of the bilinear softening curve, respectively. According to Petersson (1981), the σ_s and COD_s values can be considered using the following equations:

$$\sigma_s = \frac{1}{3} f_t, \text{ and } COD_s = \frac{2}{9} COD_c, \tag{4}$$

where COD_c is the critical crack opening displacement. In this paper, COD_c is calculated using value of fracture energy G_F determined via work-of-fracture method, see details in Simonova et al. (2018), according to this formula:

$$COD_c = \frac{3.6 G_F}{f_t}. \tag{5}$$

In case II ($COD_s \leq CTOD_c \leq COD_c$), $\sigma(CTOD_c)$ value can be determined according to the formula:

$$\sigma(CTOD_c) = \frac{\sigma_s}{COD_c - COD_s} (COD_c - CTOD_c). \tag{6}$$

Finally, the value of the load F_{ini} was determined according to equation (7). This value can be defined as the load level at the beginning of stable crack propagation from the initial crack/notch:

$$F_{ini} = \frac{4 \cdot W \cdot K_{Ic}^{ini}}{S \cdot F_1(\alpha_0) \cdot \sqrt{a_0}}, \tag{7}$$

where W is section modulus (determined as $W = 1/6 \cdot B \cdot D^2$), S is span length, and $F_1(\alpha_0)$ is geometry function according to equation (2), where α_0 (the a_0/D ratio) is used instead of α.

4. Results

The mean values (and coefficients of variation) of the selected parameters obtained using Double-*K* fracture model are summarized in Table 1: unstable fracture toughness K_{Ic}^{un}, the K_{Ic}^{ini} / K_{Ic}^{un} ratio, i.e. the ratio expressing the resistance to stable crack propagation, the critical crack opening displacement COD_c, load level at the beginning of stable crack propagation from the initial notch F_{ini} and the F_{ini} / F_{max} ratio, i.e. the ratio between the load level at the beginning of stable crack propagation and maximum load obtained during the test.

As can be seen from Table 1, the value of unstable fracture toughness is not significantly influenced by addition of hemp fibers into the geopolymer matrix. On the contrary, the resistance to stable crack propagation, in this case expressed by K_{Ic}^{ini} / K_{Ic}^{un} ratio, was increased up to 40% in the case of specimens with the hemp fibers in amount of 1%. The similar trend was observed in the case of load ratio, where the addition of hemp fibers in amount of 1% led to increase of the load ratio about 55%.

Table 1. Mean values of selected parameters (coefficients of variation in %).

Parameter	Unit	AAFAM	AAFAM_0.5	AAFAM_1.0
Fracture toughness K_{Ic}^{un}	MPa·m$^{1/2}$	0.493 (5.4)	0.503 (3.9)	0.504 (20.8)
K_{Ic}^{ini} / K_{Ic}^{un} ratio	–	0.415 (19.8)	0.510 (5.5)	0.588 (16.9)
Critical crack opening displacement COD_c	mm	0.033 (25.2)	0.056 (26.3)	0.249 (27.2)
Load level F_{ini}	N	389.8 (23.3)	482.2 (9.6)	470.7 (1.7)
F_{ini} / F_{max} ratio	–	0.477 (17.2)	0.599 (4.1)	0.740 (5.8)

For selected specimen from each set, the records of three-point bending test in form of *F–CMOD* diagrams coupled with acoustic emission results (AE counts) and outputs of Double-*K* fracture model (load level F_{ini}) are shown in the Figs. 2 to 4. The capability to observe the damage propagation in real time during the specimens loading is one of the AE measurement benefit (Ohtsu (2015)). Therefore, first occurrence of higher number of AE counts should correspond to the beginning of stable crack propagation from the initial crack/notch, which is in this case also represented by the load level F_{ini} estimated by Double-*K* model.

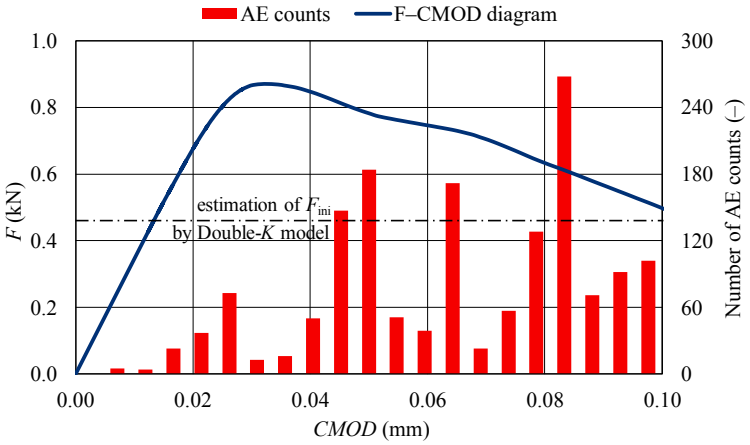

Fig. 2. *F–CMOD* diagram with AE counts for specimen AAFAM_2.

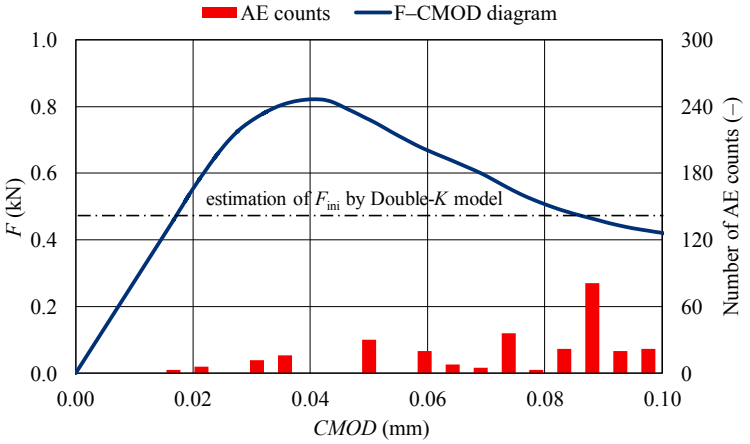

Fig. 3. *F–CMOD* diagram with AE counts for specimen AAFAM_0.5_1.

Conclusions

The aim of this study was to quantify the effect of hemp fibers on crack propagation in geopolymer mortars. From the presented experimental research results the following conclusions can be drawn:

- the resistance to stable crack propagation increased up to 40% in the case of specimens with the hemp fibers in amount of 1 %;
- the unstable crack propagation is not significantly influenced by addition of hemp fibers into the geopolymer matrix;
- the estimation of beginning of stable crack growth from initial notch by acoustic emission method is in good agreement with estimation based on Double-*K* fracture model.

The addition of fibers into alkali activated matrix should lead to reduction in the cracking tendency and improvement in tensile properties of these materials. It seems that the obtained results comply with these assumptions, but it is necessary to perform more tests to confirm these pilot results. One of the issue has to be solved is also the degradation of natural fibers in alkaline environment, therefore it is important to monitored fracture behavior during the material ageing.

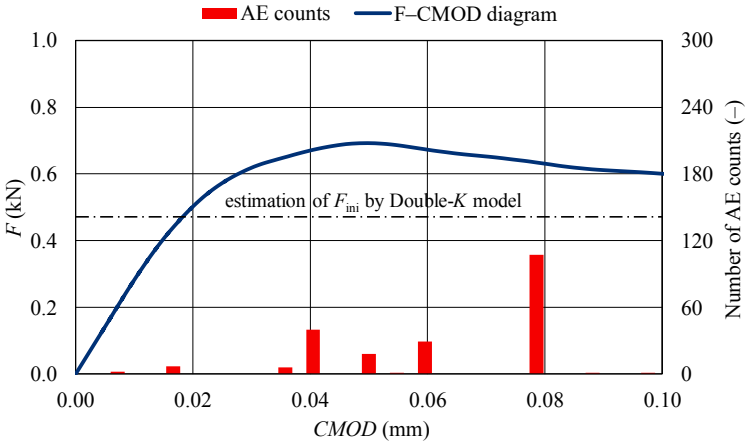

Fig. 4. *F–CMOD* diagram with AE counts for specimen AAFAM_1.0_2.

Acknowledgements

The financial support of the Czech Science Foundation, project No. 18-12289Y, is gratefully acknowledged. This outcome has been achieved with the support of projects Nos. 8J18AT009 and ID DS-2016-0060 (CZ ID 8X17060).

References

Aïtcin P. C, Mindess S., 2011. Sustainability of concrete. CRC Press, London, pp. 328.

Grosse, Ch. U., Ohtsu, M., 2008. Acoustic Emission Testing. Springer-Verlag, Berlin, pp. 416.

Komljenović, M., Baščearević, Z., Bradić, V., 2010. Mechanical and microstructural properties of alkali-activated fly ash geopolymers. Journal of Hazardous Materials 181, No. 1–3, 35–42.

Kumar, S., Barai, S. V., 2011. Concrete Fracture Models and Applications. Springer, Berlin, pp. 406.

Ohtsu, M. (Ed.) 2015.Acoustic emission and related non-destructive evaluation techniques in the fracture mechanics of concrete: fundamentals and applications. Woodhead Publishing, pp. 318.

Petersson, P. E., 1981. Crack growth and development of fracture zone in plain concrete and similar materials, Report No. TVBM-1006, Lund Institute of Technology.

Provis, J. L., van Deventer, J. S. (eds), 2014. Alkali activated materials: state-of-the-art report, RILEM TC 224-AAM. Springer, Dordrecht, pp. 388.

Reinhardt, H. W., Xu, S., 1999. Crack extension resistance based on the cohesive force in concrete. Eng. Fracture Mechanics 64, 563–587.

Sarker, P. K., Haque, R., Ramgolam, K. V., 2013. Fracture behaviour of heat cured fly ash based geopolymer concrete. Materials and Design 44 580−586.

Scrivener, K. L., John, V. M. C., Gartner, E. M., 2016. Eco-efficient cements: Potential, economically viable solutions for a low-CO_2 cement-based materials industry. United Nations Environment Programme, Paris.

Shi, C., Krivenko, P., Roy, D., 2006. Alkali-Activated Cements and Concretes. CRC Press, Taylor & Francis group, Oxon, pp. 392.

Simonova, H., Dragas, J., Kucharczykova, B., Kersner, Z., Ignjatovic, I., Komljenovic, M., Nikolic, V., 2018. Fracture Behaviour of Geopolymer Mortars Reinforced with Hemp Fibres, fib 2018 Congress, Melbourne, Australia, in print.

Šimonová, H. Lipowczan, M., Lehký, D., Kucharczyková, B., Keršner, Z., 2018. Identification of mechanical fracture parameters for estimation of statistical properties of geopolymer mortars. Beton- und Stahlbetonbau International Probabilistic Workshop 2018, in print.

Zhang, X., Xu, S., 2011. A comparative study on five approaches to evaluate double-K fracture toughness parameters of concrete and size effect analysis. Engineering Fracture Mechanics 78, 2115–2138.

Zhou, X., Kastiukas, G., 2017. Engineering Properties of Treated Natural Hemp Fiber-Reinforced Concrete. Frontiers in Building Environment 3, Article 33, 1–9.